

Calpain-Mediated Tau Cleavage: A Mechanism Leading to Neurodegeneration Shared by Multiple Tauopathies

Adriana Ferreira¹ and Eileen H Bigio^{2,3}

¹Department of Cell and Molecular Biology, ²Department of Pathology, and ³Cognitive Neurology and Alzheimer Disease Center, Feinberg School of Medicine, Northwestern University, Chicago, Illinois, United States of America

Tau dysfunction has been associated with a host of neurodegenerative diseases called tauopathies. These diseases share, as a common pathological hallmark, the presence of intracellular aggregates of hyperphosphorylated tau in affected brain areas. Aside from tau hyperphosphorylation, little is known about the role of other posttranslational modifications in tauopathies. Recently, we obtained data suggesting that calpain-mediated tau cleavage leading to the generation of a neurotoxic tau fragment might play an important role in Alzheimer's disease. In the current study, we assessed the presence of this tau fragment in several tauopathies. Our results show high levels of the 17-kDa tau fragment and enhanced calpain activity in the temporal cortex of AD patients and in brain samples obtained from patients with other tauopathies. In addition, our data suggest that this fragment could partially inhibit tau aggregation. Conversely, tau aggregation might prevent calpain-mediated cleavage, establishing a feedback circuit that might lead to the accumulation of this toxic tau fragment. Collectively, these data suggest that the mechanism underlying the generation of the 17-kDa neurotoxic tau fragment might be part of a conserved pathologic process shared by multiple tauopathies.

© 2011 The Feinstein Institute for Medical Research, www.feinsteininstitute.org

Online address: <http://www.molmed.org>

doi: 10.2119/molmed.2010.00220

INTRODUCTION

Tau dysfunction has been implicated in neuronal degeneration in several diseases known as tauopathies (1). The most common tauopathy is Alzheimer's disease (AD), but this group of pathological conditions also includes frontotemporal dementia with parkinsonism linked to chromosome 17 (FTDP-17), corticobasal degeneration (CBD), progressive supranuclear palsy (PSP), tangle-predominant senile dementia (TPSD), Pick disease (PD), dementia pugilistica (DP), and multiple system tauopathy with dementia (MSTD), among others. These diseases share, as pathological hallmarks, the presence of intracellular aggregates of hyperphosphorylated tau organized into filaments known as neurofibrillary

tangles (NFT), Pick bodies, astrocytic plaques, tufted astrocytes, and threads (2,3). Recently, a series of reports suggested that, besides phosphorylation, other posttranslational modifications might be involved in the mechanisms underlying tau pathology (4–8). Thus, we have previously shown that β -amyloid ($A\beta$) oligomers induced calpain-mediated tau cleavage leading to the generation of a 17-kDa tau fragment in cultured hippocampal neurons (9). This tau cleavage preceded tau phosphorylation in $A\beta$ -treated hippocampal neurons, suggesting that it might be an early event in the pathological process. Furthermore, our data indicated that the expression of this fragment in cultured hippocampal neurons led to their

progressive degeneration (9). Conversely, conditions that prevented the generation of this fragment were accompanied by enhanced neuronal survival in central neurons (10,11). Because calpain is a calcium-dependent protease, its activity could be dysregulated in pathological conditions associated with abnormal calcium influx, as described in AD and many other tauopathies (12–16). Together, these data suggest that the calpain-mediated generation of this neurotoxic tau fragment might be part of the pathobiology of AD, and perhaps, all tauopathies.

In the present study, we determined whether the 17-kDa tau fragment was present in brain areas affected in AD and other tauopathies. In addition, we analyzed a potential relationship between tau cleavage and tau aggregation in degenerating central neurons. Collectively, our data suggest that the mechanism underlying the generation of the 17-kDa tau fragment might be part of a conserved pathologic process shared by multiple tauopathies.

Address correspondence and reprint requests to Adriana Ferreira, Cell and Molecular Biology Department, Feinberg School of Medicine, Northwestern University, Ward Building 8-140, 303 East Chicago Avenue, Chicago, IL 60611. Phone: (312) 503-0597; Fax: (312) 503-7345; E-mail: a-ferreira@northwestern.edu.

Submitted November 20, 2010; Accepted for publication March 18, 2011; Epub (www.molmed.org) ahead of print March 21, 2011.

Table 1. Human brain tissue analyzed in this study.

Pathological diagnosis	Age at onset	Age at death	Sex	PMI, h
Control	NA	90	M	3
Control	NA	89	F	4.5
Control	NA	88	M	12
Control	NA	88	M	11
Control	NA	71	F	40
Control	NA	89	M	18
AD	68	74	M	20
AD	68	77	F	24
AD	51	64	M	12
AD	54	71	M	6
AD	77	89	F	71
AD	78	87	F	16
PSP	81	87	M	19
PSP	72	75	F	18
PSP	64	68	M	14
CBD	57	67	M	12
CBD	36	44	M	20
CBD	68	78	M	8
CBD	75	82	F	12
CBD	Unknown	93	F	22
TPSD	75	84	F	6
TPSD	83	85	F	5
PD	50	55	M	9
FTDP-17	33	36	M	19
DP	83	90	M	17
MSTD	71	74	F	8

NA, not applicable; AD, Alzheimer's disease, Braak stages V and VI.

MATERIALS AND METHODS

Preparation of Human Cortical Samples

Human cortical tissue from the superior temporal gyrus (Brodmann's area 22) obtained from control individuals (63–90 years old; cognitively intact, with maximum Braak stages I and II according to the criteria described by Braak and Braak [17]) and AD cases (64–89 years old; clinically demented and with pathologically severe AD, Braak stages V and VI) were used for the preparation of whole cell extracts (18). Extracts were also prepared from cortical tissue from patients with FTDP-17, CBD, PSP, TPSD, PD, DP, or MSTD. The post mortem interval (PMI) for all subjects ranged between 3 and 71 h, with a median value of 12 h (Table 1).

Preparation of Primary Rat Hippocampal Cultures and Treatment with Preaggregated A β

Embryonic day-18 rat embryos (euthanized by CO₂ overdose) were used to prepare primary hippocampal cultures as previously described (19,20). Briefly, hippocampi were dissected, freed of meninges, dissociated by trypsinization, and plated on poly-L-lysine-coated dishes in minimum essential medium (MEM) with 10% horse serum. After 2 h, the medium was changed to glia-conditioned MEM containing N2 supplements plus ovalbumin (0.1%) and sodium pyruvate (0.1 mmol/L) (N2 medium) (21). Twenty-one days after plating, hippocampal neurons were incubated with preaggregated A β (20 μ mol/L) as previously described (22,23). Hippocampal neurons grown in the presence of A β for 24 h were scraped in Laemmli buffer to prepare whole cell extracts (18). The Northwestern University Animal Care and Use Committee approved the experimental protocol used in this study in accordance with United States Public Health Service regulations and applicable federal and local laws.

Electrophoresis and Immunoblotting

Whole cell lysates were boiled for 10 min, and separated by sodium dodecyl sulfate (SDS)-polyacrylamide gel electrophoresis (18). Transfer of protein to Immobilon membranes (Millipore, Billerica, MA, USA) and immunodetection were performed as previously described (24). The following primary antibodies were used: tau (clone tau5; 1:1000; BioSource, Foster City, CA, USA), dephosphorylated tau (clone tau1; 1:500; Millipore), phosphorylated tau (clone AT8; 1:1000; Thermo Scientific, Rockford, IL, USA), spectrin (1:1000; Millipore), calpain 1 (1:500; Abcam, Cambridge, MA, USA), neuron-specific Class III β -tubulin (clone TUJ1; 1:4000; R&D Systems, Minneapolis, MN, USA), and α -tubulin (clone DM1A; 1:200,000; Sigma, St. Louis, MO, USA). Secondary antibodies conjugated to horseradish peroxidase (1:1000; Promega, Madison, WI) followed by en-

hanced chemiluminescence reagents were used for the detection of proteins (25). Immunoreactive bands were imaged using a ChemiDoc XRS apparatus (Bio-Rad, Hercules, CA, USA). Density of these bands was quantified using Quantity One software (Bio-Rad). Values were calculated as a ratio of the target fragment to full-length protein (tau or spectrin), and compared with the levels detected in controls (100%). Tubulin was used as a loading control.

Expression and Purification of Recombinant Full-Length and 17-kDa Tau.

To generate a Histidine-tag 17-kDa tau fragment, we used a full-length tau construct with an N-terminal 6-Histidine tag inserted into the pT7C plasmid (hT40-pT7C plasmid) as a template. The 17-kDa tau construct was generated by performing polymerase chain reaction (PCR) with the forward primer 5'-GGAATTCATATGAAAGAATCTCCCCTGCAGACC-3' and the reverse primer 5'-GCCGGAATCTTAACGGACCACTGCCACCTTCTT-3'. Recombinant proteins were purified by metal affinity chromatography on a nickel-based HisTrap FastFlow column (GE Healthcare Life Sciences, Piscataway, NJ, USA) as previously described (15). Target fractions were identified by Coomassie staining of SDS-PAGE gels, and the crude tau recombinant protein was further purified via size-exclusion chromatography using the Superdex 75 gel filtration column (GE Healthcare Life Sciences). Recombinant proteins were concentrated by use of Vivaspin 6 centrifugal concentrators (Vivaproducts, Littleton, MA, USA), and protein concentration was determined as previously described (26,27). Recombinant proteins were characterized by Western blot analysis using the following antibodies: tau (clone tau5; 1:1000; BioSource), N-terminal tau (1:2000; Chemicon, Temecula, CA, USA), C-terminal tau (clone T46; 1:2500; Zymed, San Francisco, CA, USA), and polyhistidine (1:6000; Sigma). Electro-spray ionization Fourier transform mass spectrometry was performed to confirm

the molecular weight of the novel recombinant 17-kDa tau protein.

Fluorescence-Based Aggregation Studies

Full-length tau (4 μmol/L) was aggregated alone or in the presence of the 17-kDa tau fragment (4 μmol/L) by incubating these proteins with 150 μmol/L arachidonic acid (AA; Cayman Chemical, Ann Arbor, MI, USA) in polymerization buffer (5 mmol/L DTT, 100 mmol/L sodium chloride, 10 mmol/L HEPES, pH 7.6) for 5 h at room temperature as previously described (28,29). Polymerization was monitored by adding Thioflavine S (ThS) at a final concentration of 20 μmol/L and measuring fluorescence (excitation of 440 nm and emission of 520 nm) in the Infinite M200 microplate reader (Tecan, Männedorf, Switzerland) as previously described (29). Data were normalized by using a negative control (polymerization buffer alone). Data were analyzed and fit by nonlinear regression to single phase exponential association equations by using GraphPad PRISM (La Jolla, CA, USA).

Electron Microscopy

Full-length tau was allowed to aggregate for 20 h following induction with AA in either the presence or the absence of the 17-kDa tau fragment. Samples were then fixed in 2% glutaraldehyde for 10 min, loaded onto Formvar/carbon coated copper grids (Electron Microscopy Sciences, Fort Washington, PA, USA) and negatively stained with 2% uranyl acetate for 1 min as previously described (30). Grids were prepared in duplicate from three independent experiments and visualized with a JEOL JEM-1220 electron microscope. Filament length was determined and total number of fibrils counted to assess density by using the image analysis software MetaMorph (Molecular Devices, Downingtown, PA, USA). The average filament mass of each field was calculated by multiplying the average length of filaments by the number of filaments per field.

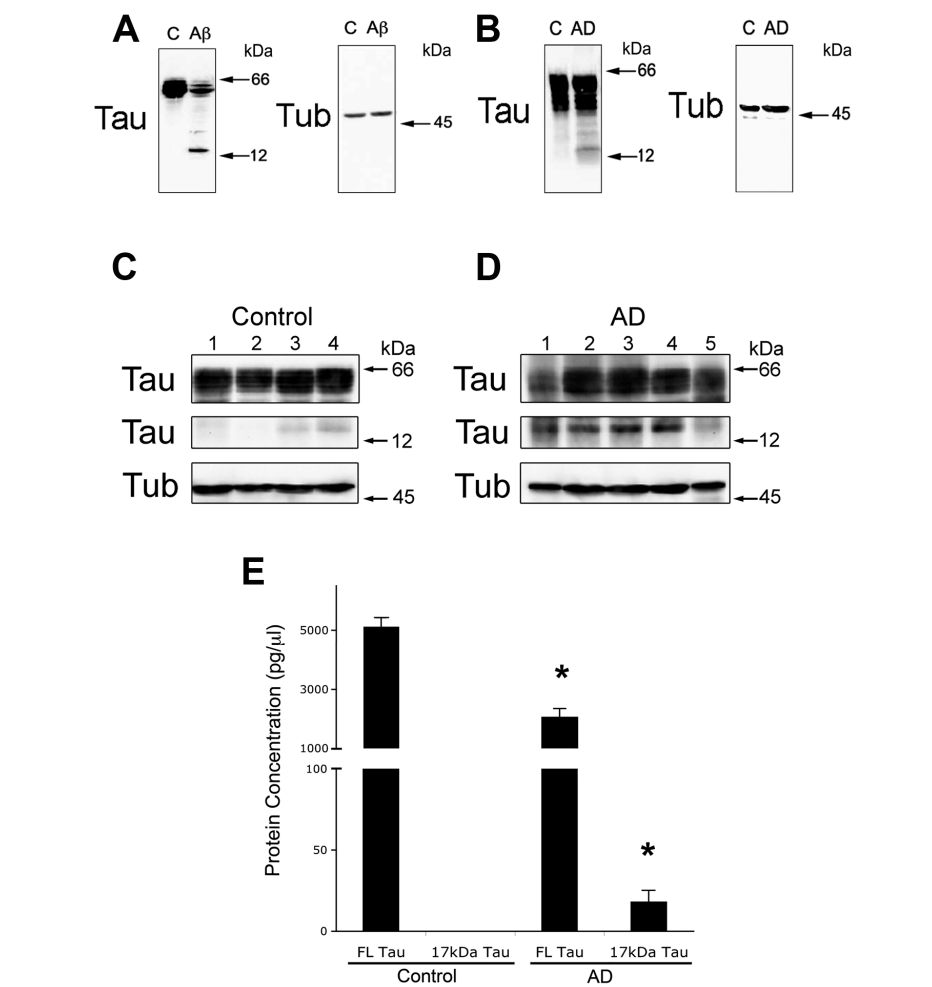


Figure 1. The 17-kDa tau fragment was detected in AD brain samples. (A) Quantitative Western blot analysis of tau content in whole cell lysates prepared from 21 d in culture hippocampal neurons incubated in the absence (C) or presence of aggregated Aβ (Aβ) for 24 h. Note the strong tau immunoreactive band at 17-kDa apparent molecular weight in Aβ-treated neurons. Tubulin was used as a loading control. (B) Quantitative Western blot analysis of tau content in representative whole cell lysates prepared from postmortem samples of temporal cortex from control subjects (C) and subjects with severe AD (AD). (C–E) Full-length tau and 17-kDa tau fragment levels in whole cell lysates prepared from postmortem samples of temporal cortex from control subjects (C) and subjects with severe AD (D). Numbers in (E) represent the mean ± SEM. Differs from control, *P < 0.05.

In Vitro Calpain Studies

Full-length tau was aggregated for 5 h as described above, while soluble tau was simultaneously incubated with ethanol vehicle. Both filamentous and soluble full-length tau were then digested for 1 h at 30°C with calpain (6 μg tau/calpain unit). The cleavage reaction was stopped by the addition of an equivalent volume of Laemmli buffer and immediately boiled for 10 min. Samples were then

subjected to Western blot analysis for detection of the 17-kDa tau fragment using the tau5 antibody as described above.

Cultured hippocampal neurons were treated with or without okadaic acid (Sigma) at a final concentration of 25–100 nmol/L for 1 h. The cells were then incubated on ice for 1 h in 75 μL lysis buffer (150 mmol/L sodium chloride, 5 mmol/L ethylene glycol-bis(2-amino-ethyl ether)-N,N,N',N'-tetraacetic

acid [EGTA]; 5 mmol/L ethylenediamine-tetraacetic acid; 20 mmol/L Tris-hydrochloric acid, pH 7.4; 1% TritonX-100), after which the membranes were spun down by centrifugation at 16,000g for 10 min. The tau-containing supernatant was removed and incubated with 0.55 U calpain per 35 μ L lysate for 1 h at 30°C. An equivalent volume of Laemmli was added and samples were immediately boiled for 10 min to stop the reaction. The cleavage products were run on SDS gels as described above.

Statistical Analysis

Human samples obtained from control subjects ($n = 5$) and patients with AD ($n = 5$), PSP ($n = 3$), and CBD ($n = 5$) as well as all experiments performed in this study (at least five samples per condition) were statistically analyzed. The compiled data were analyzed by using one-way ANOVA followed by Tukey least significant difference post hoc test. The values in the graphs represent the mean \pm SEM, and statistical significance is indicated in the graphs for samples that differed from their respective controls.

RESULTS

The 17-kDa Neurotoxic Tau Fragment Was Detected in the Cortex of Patients with AD and Other Tauopathies

We have previously shown that the incubation of cultured hippocampal neurons in the presence of A β oligomers resulted in calpain-mediated tau cleavage leading to the generation of a 17-kDa neurotoxic tau fragment (9–11; see also Figure 1A). To assess the presence of this tau fragment in AD brains, whole cell lysates were prepared from samples from control individuals and patients with AD. In control cases, immunoblotting using phosphorylation-independent tau antibodies demonstrated immunoreactive bands corresponding to full-length tau and the absence of a distinct immunoreactive band at the 17-kDa apparent molecular weight (Figure 1B). Full-length tau was also easily detected in AD samples. In

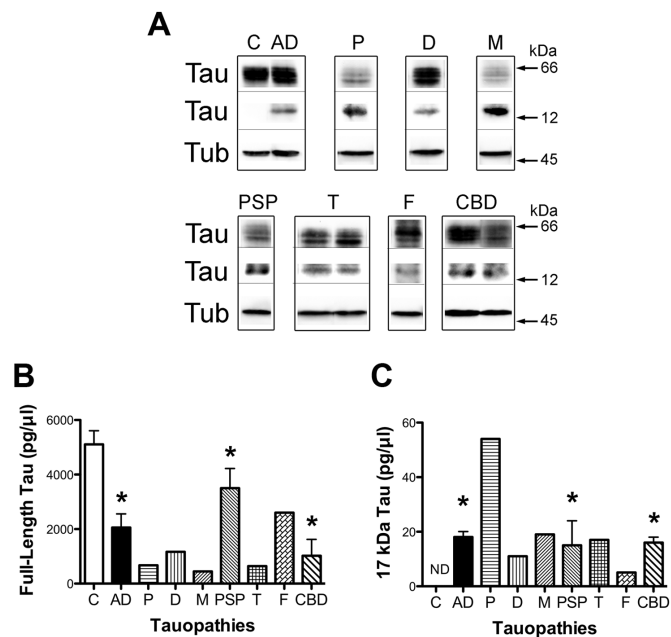


Figure 2. The 17-kDa tau fragment was also detected in the brains of patients with other tauopathies. (A) Selected representative lanes of Western blot analysis of tau content in whole cell lysates prepared from postmortem cortical samples from subjects with AD, Pick disease (P), dementia pugilistic-like neurofibrillary tangle pathology (D), multiple system tauopathy with presenile dementia (M), progressive supranuclear palsy (PSP), tangle-predominant senile dementia (T), frontotemporal dementia with parkinsonism-17 (F), corticobasal degeneration (CBD), and aged-matched controls (C). Membranes were reacted using a tau antibody (clone tau 5) and then stripped and reprobed using a tubulin antibody (clone DM1A). (B) Full-length tau and (C) 17-kDa tau fragment levels in AD and other tauopathies samples. Numbers represent the mean \pm SEM. *Differs from control, $P < 0.05$. ND, not detectable.

contrast to controls, a strong immunoreactive band corresponding to the 17-kDa tau fragment was detected in AD brain extracts (Figure 1B). Quantification of these immunoreactive bands showed a significant increase (~18-fold) in the ratio of 17-kDa/full-length tau in samples from AD patients compared with samples from age-matched controls. We next determined the levels of full-length tau and 17-kDa tau in these samples. For these experiments, Western blots were run using purified recombinant full-length tau and 17-kDa tau as standards. Our results showed a significant decrease in full-length tau and a significant increase in 17-kDa tau in AD cases compared with age-matched controls (Figure 1C–E).

We next assessed whether this fragment was also present in brain samples

obtained from patients suffering from other tauopathies. Western blot analysis of these lysates revealed a general decrease in full-length tau immunoreactivity when compared with control cases (Figure 2A). In addition, a distinct tau immunoreactive band was detected at 17-kDa apparent molecular weight in all samples analyzed (Figure 2A). Densitometric analysis of tau immunoreactive bands demonstrated an increase (ranging from ~10- to ~50-fold) in the 17-kDa/full-length tau ratio in all disease samples tested when compared with age-matched controls. As in the case of AD brains, full-length tau levels were significantly decreased, whereas the concentration of the 17-kDa tau was significantly increased in samples obtained from patients suffering from other tauopathies as compared with controls (Figure 2B, C).

To rule out a potential effect of the PMI in the production of this fragment, we calculated a correlation coefficient between PMI and 17-kDa tau levels for all samples used in this study. We found no significant correlation ($R^2 = 0.051$, $P = 0.44$) between PMI and 17-kDa tau levels in the brain samples analyzed. These results suggested that the increased 17-kDa tau levels observed in the pathological brains could not be explained by variation in the PMI.

High Levels of the 17-kDa Tau Fragment Correlated with Enhanced Calpain Activity in Patients with AD and Other Tauopathies

Previous studies have shown that the tau cleavage leading to the generation of the 17-kDa fragment was the result of calpain activation (9–11). Therefore, we next determined the extent of calpain activation in brain samples obtained from AD cases and from patients suffering from other tauopathies. For these experiments, we assessed calpain activation by determining spectrin cleavage (see also 9,31). Spectrin degradation is highly sensitive to calpain activation and considered an excellent marker for this protease activity (32). Furthermore, we have shown no significant differences when calpain activity was determined by calpain assays or by use of spectrin cleavage as a marker (9). Western blot analysis of whole cells extracts obtained from control samples using a specific spectrin antibody showed immunoreactivity primarily at 240 kDa. In contrast, a significant decrease in this immunoreactive full-length spectrin band and a concomitant increase in the calpain-dependent 150-kDa degradation fragment was detected in AD samples (Figure 3). Quantitative analysis of immunoreactive bands showed a significant increase in the spectrin 150:240 kDa ratio in AD brain samples compared with age-matched controls (Figure 3). A similar pattern was detected when samples obtained from patients suffering from other tauopathies were analyzed (Figure 3C, E).

A linear regression analysis was performed to assess a potential correlation

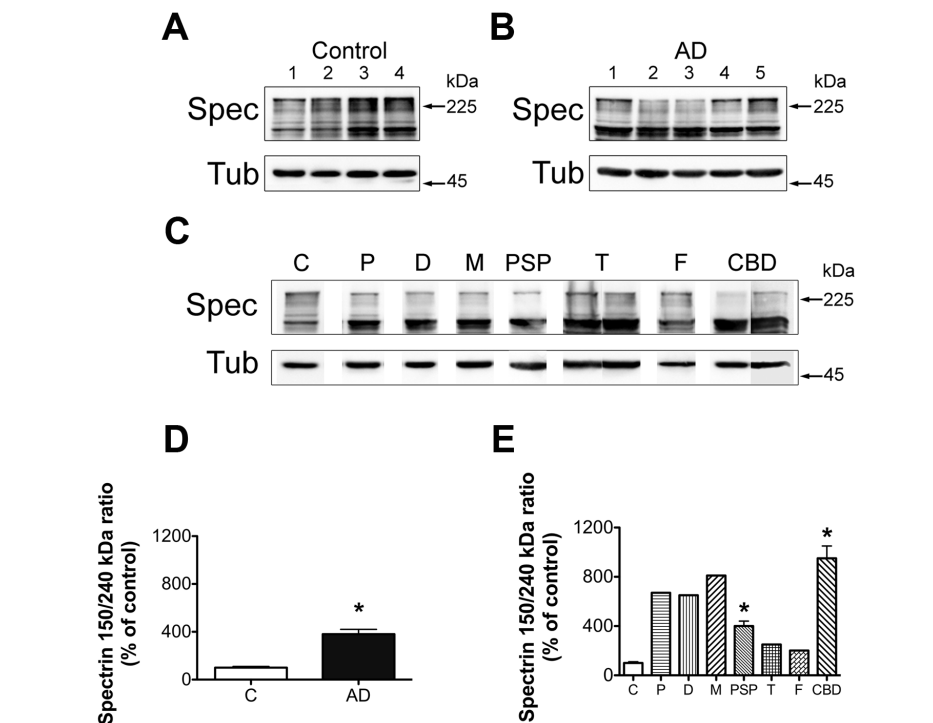


Figure 3. Determination of calpain activity using spectrin cleavage as a surrogate marker for this protease activity in AD and other tauopathy brain samples. (A–C) Western blot analysis of spectrin content in whole cell lysates prepared from postmortem samples of temporal cortex from control subjects (A), subjects with severe AD (Braak stage V–VI) (B), and subjects with other tauopathies (C). (D,E) Graphs showing the ratios of cleaved/full-length spectrin in controls, AD subjects (D), and subjects with other tauopathies (E). Numbers represent the mean \pm SEM. Values are expressed as percentage of controls, considering the values obtained in control subjects as 100%. *Differs from control subjects; $P < 0.05$.

between the levels of 17-kDa tau and calpain activity (assessed by spectrin cleavage) in the brain samples analyzed. Significant correlation was found between these two parameters, indicating that an increase in calpain activity might account, at least in part, for increased 17-kDa tau in these subjects ($R^2 = 0.41$, $P = 0.006$). A similar analysis showed no significant correlation between PMI and the spectrin 150:240 kDa ratio, ruling out that the activation of this protease was regulated by variations in PMI ($R^2 = 0.021$, $P = 0.62$).

To assess to what extent the increase in calpain activity seen in patients with AD and other tauopathies was due to increased levels of this protease, we performed quantitative Western blot analysis of whole cell lysates obtained from control subjects and patients with AD using a calpain antibody. Immunoblot-

ting revealed strong calpain-reactive bands at ~80 kDa in both control and AD subjects (Figure 4A, B). Variations in the immunoreactive calpain bands were detected among different samples. However, the quantification of these bands did not detect significant differences in calpain levels when AD brain lysates were compared with controls (Figure 4D). Similar results were obtained using samples prepared from other tauopathies patients (Figure 4E).

The 17-kDa Tau Fragment Inhibited Aggregation of Full-Length Tau Into Filaments *In Vitro*.

Because tauopathies share, as a common pathological hallmark, the presence of characteristic insoluble tau aggregates, we investigated a potential relationship between tau cleavage and tau aggrega-

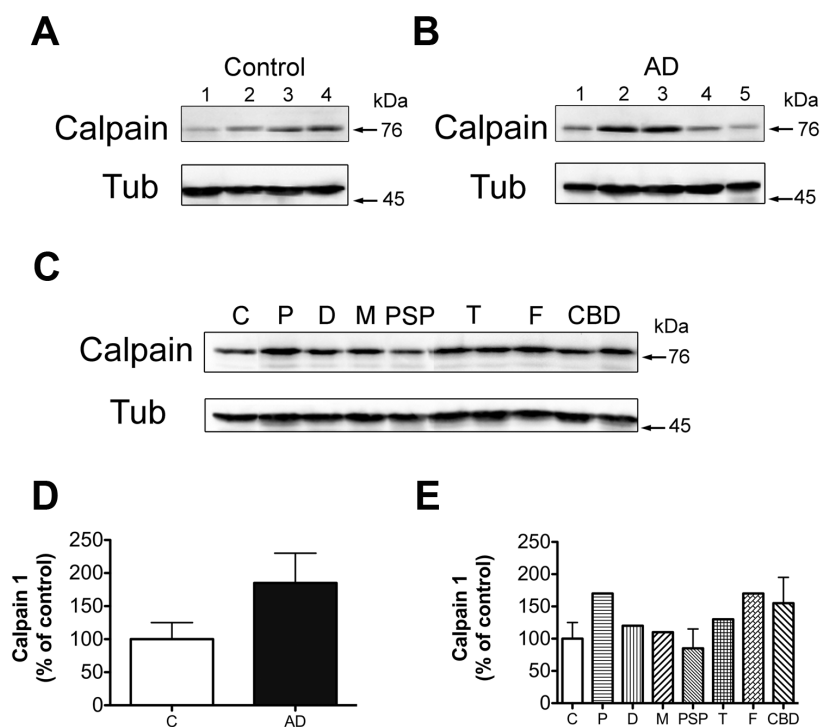


Figure 4. Calpain levels did not differ in control, AD, and other tauopathy cases. (A–C) Western blot analysis of calpain content in whole cell lysates prepared from postmortem samples of temporal cortex from control subjects (A), subjects with severe AD (Braak stage V–VI) (B) and subjects with other tauopathies (C). (D,E) Graphs showing calpain levels in controls, AD subjects (D), and subjects with other tauopathies (E). Numbers represent the mean \pm SEM of control subjects in lanes 1–4, AD subjects in lanes 1–5, PSP and CBD or the mean densitometry value of each of the other disease groups. Values are expressed as percentage of controls, considering the values obtained in control subjects as 100%.

tion. We determined first whether 17-kDa tau might play a role in full-length tau polymerization. For these experiments, we generated a recombinant construct consisting of 17-kDa tau with an *N*-terminal polyhistidine tag. This construct was then characterized with a battery of antibodies. As expected, recombinant 17-kDa tau was highly immunoreactive with clone tau5 directed to an epitope spanning amino acids 210–230, but failed to react with antibodies to either the extreme *N*- or *C*-termini of tau (Figure 5A). The calculated weight of the amino acid sequence of 17-kDa tau with the 6 polyhistidine tag is 21 kDa (Figure 5A). The mass of this protein was confirmed by electrospray ionization Fourier transform mass spectrometry (Figure 5B).

To analyze the role of 17-kDa tau in the formation of full-length tau fila-

ments, we induced aggregation using 150 μ mol/L AA. These studies were performed using a 1:1 molar ratio because this approach has been successfully used to test the effects of other tau fragments on full-length tau aggregation (7). Incubation of full-length tau (4 μ mol/L) with AA induced aggregation as detected by means of ThS fluorescence, which followed a single-phase exponential equation association curve (33–35). When both tau constructs were mixed together in a 1:1 molar ratio, the resultant fluorescent output was significantly lower than when ht40 was aggregated alone (Figure 5C). These results suggested that 17-kDa tau was capable of reducing the polymerization of full-length tau.

To further evaluate the apparent inhibition of full-length polymerization, we examined filament formation when 4

μ mol/L full-length tau was aggregated in the presence or absence of 4 μ mol/L 17-kDa tau by means of electron microscopy. As the *in vitro* aggregation experiments suggested, electron microscopy micrographs showed fewer filaments when full-length tau was aggregated in the presence of 17-kDa tau compared with full-length tau aggregated alone (Figure 6A, B). Filament length remained unchanged, with each type of polymerization reaction showing a mixture of short and long filaments. Quantification of these filaments revealed a significant decrease in the number of filaments/square micron in full-length tau aggregated with 17-kDa tau when compared with full-length tau aggregated alone (Figure 6C). Because the average length of filaments was similar between full-length tau aggregated in the absence and presence of 17-kDa tau (Figure 6D), the reduction in filament number caused by coincubation with 17-kDa tau led to a decline in average filament mass (Figure 6E).

The Aggregation of Full-Length Tau into Filaments as well as Its Phosphorylation Decreased Its Vulnerability to Calpain Proteolysis and Subsequent Generation of the 17-kDa Tau Fragment

Results of previous studies have suggested that because of its fibrillary conformation aggregated tau is less susceptible to protease cleavage (36,37). However, no information is available regarding the generation of specific cleavage products when aggregated tau is exposed to calpain. To assess whether polymerized full-length tau indeed has differential susceptibility to the production of the 17-kDa fragment, we performed *in vitro* calpain cleavage assays. Recombinant full-length tau was aggregated for 5 h after induction with AA, as described above. These aggregates, as well as soluble tau, were then incubated in the presence or absence of calpain for 1 h at 30°C, followed by Western blot analysis. Aggregation was further verified by the presence of high molecular weight species absent from soluble tau (Figure 6F, lanes 2 and 4). In the

absence of calpain, the 17-kDa fragment was virtually undetectable in either aggregated or unaggregated tau samples. Similarly, very little tau immunoreactivity was detected at 17 kDa in samples of polymerized tau treated with calpain (Figure 6F, lane 4). In contrast, incubation of soluble tau with calpain generated a strong immunoreactive band at 17-kDa (Figure 6F, lane 3).

Finally, we analyzed whether enhanced tau phosphorylation also affected calpain-mediated proteolysis. For these experiments, cultured hippocampal neurons were incubated in the presence of the protein phosphatase inhibitor okadaic acid (25 and 100 nmol/L final concentrations) for 1 h. Enhanced tau phosphorylation was verified by Western blot analysis using a phosphorylation-dependent tau antibody (clone AT8; see the Materials and Methods section). As previously described, quantitative Western blot analysis showed a significant increase in tau phosphorylation in hippocampal neurons treated with okadaic acid (4884% \pm 167% and 5922% \pm 107% increases in 25 nmol/L and 100 nmol/L okadaic acid-treated neurons, respectively) when compared with untreated controls (100%). Lysates were then incubated in the presence of active calpain, and the final proteolytic products were analyzed by Western blotting. Tau present in untreated hippocampal neurons was almost completely degraded in the presence of active calpain (Figure 7). On the other hand, a full-length tau immunoreactive band was clearly detected in samples obtained after the incubation with 25 nm okadaic acid. A stronger immunoreactive band for full-length tau was also present in samples obtained from neurons treated with 100 nmol/L okadaic acid and incubated in the presence of active calpain (Figure 7).

DISCUSSION

The data presented here indicated that calpain-mediated tau cleavage leading to the generation of the 17-kDa neurotoxic tau fragment is a conserved cellular

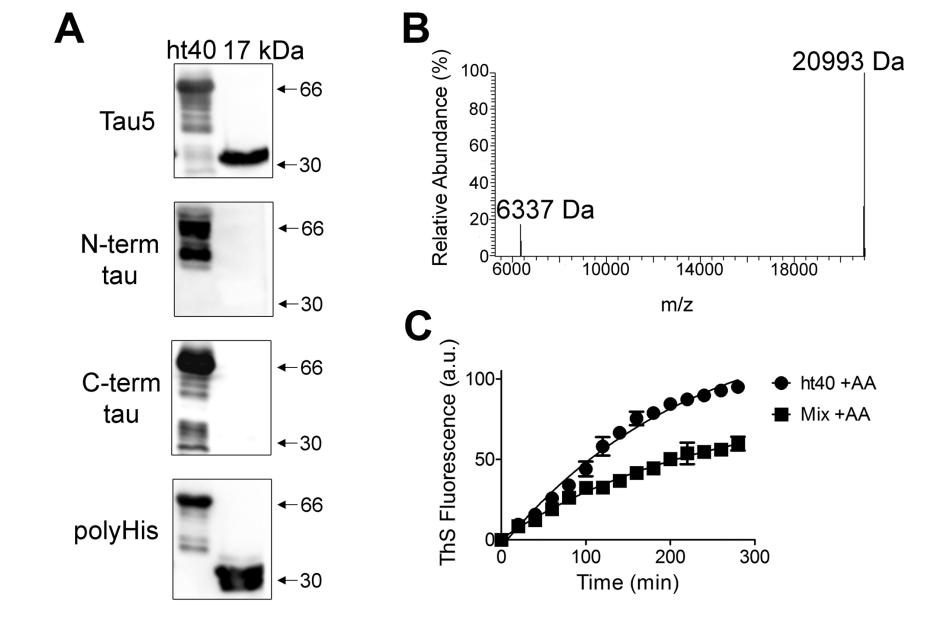


Figure 5. Decreased full-length tau polymerization in the presence of the 17-kDa fragment. (A) Immunodetection of polyhistidine-tagged recombinant ht40 and 17-kDa tau using antibodies against epitopes located in central region, (clone tau 5), the N-terminus of tau (clone T46), as well as the polyhistidine tag on both proteins. Numbers to the right of immunoblots represent apparent molecular weight. Although the band for the 17-kDa tau fragment with polyhistidine migrates at approximately 32 kDa, mass spectroscopy demonstrated that the mass of the purified protein is the expected 21 kDa with negligible contamination (B). (C) ThS (20 μ mol/L final concentration) was used to follow the kinetics of polymerization of 4 μ mol/L ht40 alone or in the presence of 17-kDa tau (1:1 mixture). Results are the average of five independent experiments and error bars represent the SEM. End-point analysis (time = 300 min) indicated an inhibition of polymerization of ht40 by the addition of 4 μ mol/L 17-kDa tau ($P < 0.01$).

event shared by many tauopathies. Furthermore, they provided insights into a feedback circuit between this cleavage and tau aggregation, a mechanism that might have some bearings in the pathobiology of these diseases.

The role of tau phosphorylation in AD has been extensively studied because neurofibrillary tangles (NFT) are intracellular aggregates of hyperphosphorylated forms of this MAP (20,22,30,38–51). On the other hand, little is known about the potential effects of other tau posttranslational modifications on neuronal survival in AD. Emerging evidence suggests that calpain-mediated tau cleavage leads to the generation of the 17-kDa neurotoxic fragment in a dose- and time-dependent manner (9–11). On the basis of these data, it is tempting to speculate that this cleaved product could contribute to tau-

mediated toxicity, if present in neurons undergoing degeneration *in situ*. The data presented here provide the first evidence of the presence of this tau fragment in brain samples obtained from AD cases. The proteolytic activity underlying the generation of this fragment could have taken place as the neurodegenerative process progressed in the affected brain areas of these patients. Alternatively, tau cleavage could be the result, at least in part, of the postmortem activation of proteases. However, the lack of a significant correlation between the levels of this fragment and the PMI before these brain samples were obtained ruled out a nonspecific postmortem degradation process as a significant contributor to the generation of the 17-kDa tau fragment in AD and other tauopathies. Together, these data identified this tau

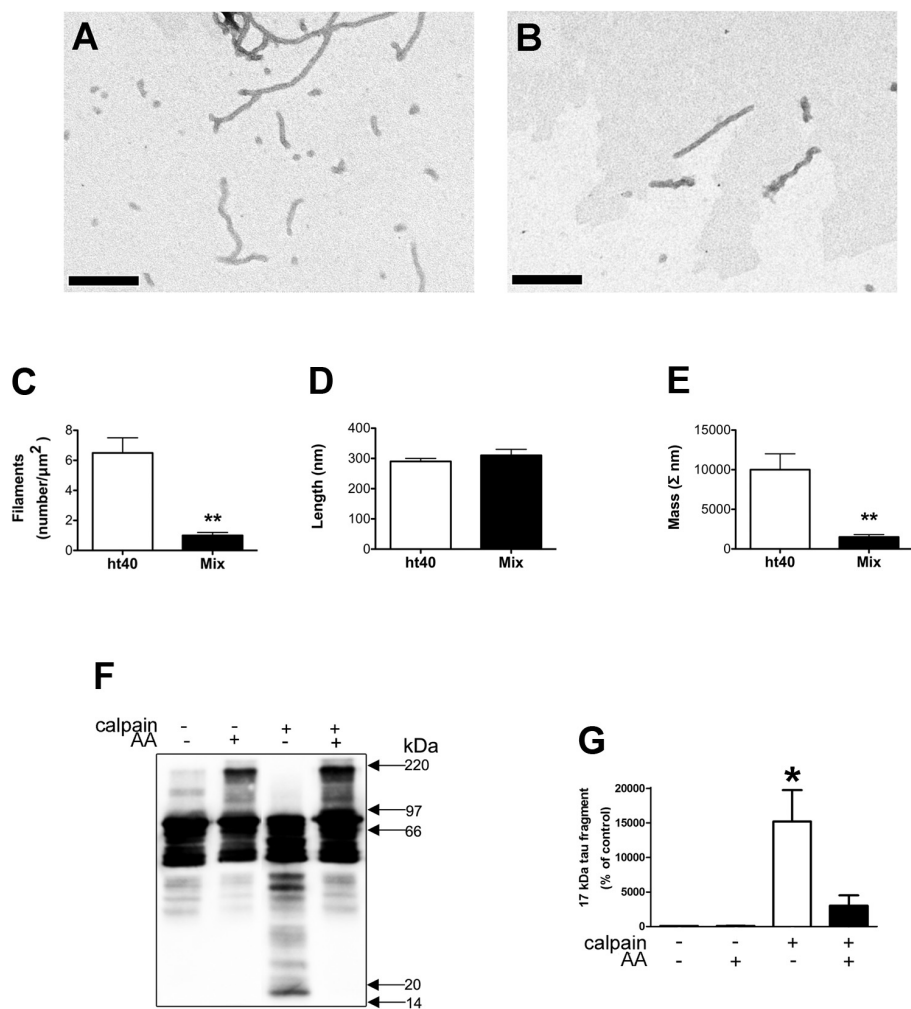


Figure 6. Polymerization of full-length tau decreased in the presence of the 17-kDa tau fragment, increasing its susceptibility to calpain cleavage. (A,B) Negative stain electron micrographs of filaments of hT40 (4 $\mu\text{mol/L}$) polymerized with AA in the absence (A) or presence (B) of 17-kDa tau (4 $\mu\text{mol/L}$). (C-E) Graphs showing the number (C), length (D), and mass (E) of filaments formed by full-length tau in the presence or absence of the 17-kDa tau fragment. Numbers represent the mean \pm SEM from five independent experiments (** $P < 0.01$). Bars = 200 nm. (F) Western blot analysis of full-length tau (hT40) induced to aggregate (AA+) or allowed to remain in its native state (AA-) and then incubated in the presence or absence of active calpain. (G) Graph showing the difference in production of the 17-kDa tau fragment under the experimental conditions shown in A. Each number represents the mean \pm SEM from five independent experiments. *Differs from all other experimental conditions, $P < 0.05$.

cleavage as the first posttranslational modification of tau, other than phosphorylation, shared by multiple tauopathies.

Tau cleavage correlated with increased calpain activity, but not increased levels of this protease, when AD and other tauopathy cases were compared with aged-matched controls. These results are in agreement with previous reports

showing widespread activation of calpain in frontal cortex of AD-affected individuals (reviewed in 54,55). Because calpain is a calcium-dependent protease, the enhanced calpain activity detected in the brains of AD cases could have been triggered by disturbances in calcium influx. Abnormalities in calcium homeostasis have already been described as

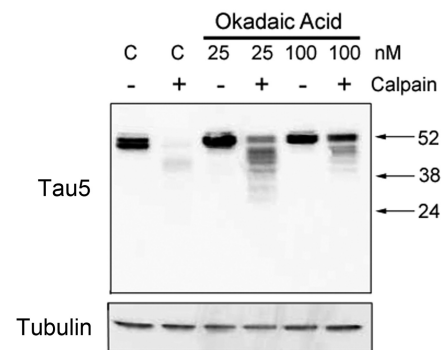


Figure 7. Decreased susceptibility of hyperphosphorylated full-length tau to calpain cleavage. Western blot analysis of whole cell extracts obtained from untreated hippocampal neurons (c) and neurons treated with 25 or 100 nmol/L okadaic acid and then incubated in the presence (+) or absence (-) of active calpain. Membranes were reacted with a tau antibody (clone tau 5) and then stripped and reprobbed with a tubulin antibody as a loading control. Note that the treatment with okadaic acid decreased the susceptibility of tau to calpain cleavage in a dose-dependent manner.

associated with A β accumulation, excitotoxicity, and response to brain injury (54,56,57). Our data are also in agreement with insights into the molecular mechanisms leading to the generation of this neurotoxic fragment obtained using cultured hippocampal neurons treated with aggregated A β and a transgenic mouse model of this disease (9-11,31). Those studies indicated that A β induced the abnormal activation of calpain through enhanced and sustained calcium influx mediated by N-methyl-D-aspartate (NMDA) receptors and not by an increase in the protein levels of this protease (9,31,58).

Recently, other mechanisms have been implicated in the activation of calpains. Thus, it has been shown that calpain 2, but not calpain 1, was activated by ERK-mediated phosphorylation under certain experimental conditions (59,60,61). Because the ERK signal transduction pathway is highly activated in the presence of A β in mature central neurons, it is possible that this mechanism could play a role in the generation of the 17-kDa tau in AD

(20,22). However, this seems not to be the case in view of our previous results showing that NMDA antagonists completely blocked calpain activation and the production of this tau fragment in A β -treated neurons (62).

A decrease in the levels of calpastatin, a calpain endogenous inhibitor, could contribute to the abnormal activation of this protease observed in brain samples from patients with AD and from patients with other tauopathies (58,63). Recently, it has been shown that calpastatin levels decreased as the AD pathological process progressed (64). Calpastatin decrease has been attributed to the proteolytic activity of caspase 3 and calpain (64). Together, these data suggest that calcium homeostasis dysregulation might lead to the initial enhanced activation of calpain. In turn, the abnormal activation of this protease could then be perpetuated by calpastatin depletion due to its cleavage by calpain and caspase 3.

Regardless of the mechanisms underlying the abnormal calpain activity, the presence of this 17-kDa tau neurotoxic fragment in different tauopathies suggests that it might play a role in the mechanisms underlying neuronal degeneration in these diseases. We have previously shown that the expression of this fragment, in otherwise healthy neurons, resulted in the progressive degeneration leading to cell death, indicating that the 17-kDa tau fragment has intrinsic toxic effects (9–11). More recently, a tau fragment of similar molecular weight was found to be nontoxic when expressed in a neuroblastoma cell line or in younger cultured hippocampal neurons (65). This apparent discrepancy could be due to several factors including, but not limited to, differences in the aged of the cultured hippocampal neurons, the culture conditions (that is, presence of glial cells, culture medium, etc.), and/or in the levels of expression of the 17-kDa tau under the different experimental conditions used by these authors. Alternatively, these fragments could be slightly different because the fragment studied by Wang *et al.* was the result of cleavage of calpain 2 and not

calpain 1, as was the 17-kDa tau fragment described by our result group.

Although further studies will be required to determine the molecular mechanisms underlying the toxic effects of the 17-kDa tau fragment, the results described above provide some insights into both the potential role of this fragment in tau aggregation and the role of enhanced phosphorylation in the generation of this fragment. The complete elucidation of the mechanisms underlying the relationship between this cleavage and tau phosphorylation and aggregation in the context of these neurodegenerative disorders awaits further investigation.

ACKNOWLEDGMENTS

This work was supported by NIH grants R01 NS39080 to A Ferreira and P30 AG13854 to EH Bigio. Proteomics and informatics services were provided by the CBC-UIC Research Resources Center Proteomics and Informatics Services Facility funded by a grant from the Searle Funds at the Chicago Community Trust to the Chicago Biomedical Consortium. The authors thank Sara Kleinschmidt, who participated in the early stages of this study.

DISCLOSURE

The authors declare that they have no competing interests as defined by *Molecular Medicine*, or other interests that might be perceived to influence the results and discussion reported in this paper.

REFERENCES

1. Yancopoulos D, Spillantini MG. (2003) Tau protein in familial and sporadic diseases. *Neuromol. Med.* 4:37–48.
2. Gotz J. (2001) Tau and transgenic animal models. *Brain. Res. Rev.* 35:266–86.
3. Lee VM, Goedert M, Trojanowski JQ. (2001) Neurodegenerative tauopathies. *Annu. Rev. Neurosci.* 24:1121–59.
4. Gambin TC, *et al.* (2003a) Caspase cleavage of tau: linking amyloid and neurofibrillary tangles in Alzheimer's disease. *Proc. Natl. Acad. Sci. U. S. A.* 100:10032–37.
5. Guo H, *et al.* (2004) Active caspase-6 and caspase-6 cleaved tau in neuropil threads, neuritic plaques, and neurofibrillary tangles of Alzheimer's disease. *Am. J. Pathol.* 165:523–31.
6. Horowitz PM, LaPointe N, Guillozet-Bongaarts AL,

7. Berry RW, Binder LI. (2006) N-terminal fragments of tau inhibit full-length tau polymerization in vitro. *Biochem.* 45:12859–66.
8. Reynolds MR, Berry RW, Binder LI. (2005) Site-specific nitration and oxidative dityrosine bridging of the tau protein by peroxynitrite: implications for Alzheimer's disease. *Biochem.* 44:1690–00.
9. Reynolds MR, Lukas TJ, Berry RW, Binder LI. (2006) Peroxynitrite-mediated tau modifications stabilize preformed filaments and destabilize microtubules through distinct mechanisms. *Biochem.* 45:4314–26.
10. Park SY, Ferreira A. (2005) The generation of a 17 kDa neurotoxic fragment: an alternative mechanism by which tau mediates beta-amyloid-induced neurodegeneration. *J. Neurosci.* 25:5365–75.
11. Park SY, Tournell C, Sinjoanu RC, Ferreira A. (2007) Caspase-3- and calpain-mediated tau cleavage are differentially prevented by estrogen and testosterone in beta-amyloid-treated hippocampal neurons. *Neurosci.* 144:119–27.
12. Sinjoanu RC, *et al.* (2008) The novel calpain inhibitor A-705253 potentially inhibits oligomeric beta-amyloid-induced dynamin 1 and tau cleavage in hippocampal neurons. *Neurochem. Intl.* 53:79–88.
13. Adamec E, Mohan P, Vonsattel JP, Nixon RA. (2002) Calpain activation in neurodegenerative diseases: confocal immunofluorescence study with antibodies specifically recognizing the active form of calpain 2. *Acta. Neuropathol.* 104:92–104.
14. Albers DS, Beal MF. (2002) Mitochondrial dysfunction in progressive supranuclear palsy. *Neurochem. Intl.* 40:559–64.
15. LaFerla FM. (2002) Calcium dyshomeostasis and intracellular signaling in Alzheimer's disease. *Nat. Rev. Neurosci.* 3:862–72.
16. Furokawa K, *et al.* (2003) Alteration in calcium channel properties is responsible for the neurotoxic action of a familial frontotemporal dementia tau mutation. *J. Neurochem.* 87:427–36.
17. Xie CW. (2004) Calcium-regulated signaling pathways: role in amyloid beta-induced synaptic dysfunction. *Neuromol. Med.* 6:53–64.
18. Braak H, Braak E. (1991) Neuropathological staging of Alzheimer-related changes. *Acta. Neuropathol.* 82:239–59.
19. Laemmli UK. (1970) Cleavage of structural proteins during the assembly of the head of bacteriophage T4. *Nature.* 227:680–85.
20. Goslin K, Banker GA. (1991) Rat hippocampal neurons in low-density culture. In: *Culturing Nerve Cells*. Banker G, Goslin K (eds). MIT Press, Cambridge, pp. 251–83.
21. Ferreira A, Lu Q, Orecchio L, Kosik KS. (1997) Selective phosphorylation of adult tau isoforms in mature hippocampal neurons exposed to fibrillar A beta. *Mol. Cell. Neurosci.* 9:220–34.
22. Bottenstein JE, Sato GH. (1979) Growth of a rat neuroblastoma cell line in serum-free supplemented medium. *Proc. Natl. Acad. Sci. U. S. A.* 76:514–17.
23. Rapoport M, Ferreira A. (2000) PD98059 prevents neurite degeneration induced by fibrillar beta

- amyloid in mature hippocampal neurons. *J. Neurochem.* 74:125–33.
23. Rapoport M, Dawson HN, Binder LI, Vitek MP, Ferreira A. (2002) Tau is essential to beta-amyloid-induced neurotoxicity. *Proc. Natl. Acad. Sci. U. S. A.* 99:6364–69.
 24. Towbin H, Staehelin T, Gordon J. (1979) Electrophoretic transfer of proteins from polyacrylamide gels to nitrocellulose sheets: procedure and some applications. *Proc. Natl. Acad. Sci. U. S. A.* 76:4350–54.
 25. Yakunin AF, Hallenbeck PC. (1998) A luminol/iodophenol chemiluminescent detection system for Western immunoblots. *Anal. Biochem.* 258:146–49.
 26. Lowry OH, Rosebrough NJ, Farr AL, Randall RJ. (1951) Protein measurement with the Folin phenol reagent. *J. Biol. Chem.* 193:265–75.
 27. Bensadoun A, Weinstein D. (1976) Assay of proteins in the presence of interfering materials. *Anal. Biochem.* 70:241–50.
 28. Carlson SW, et al. Carlson SW, et al. (2007) A complex mechanism for inducer mediated tau polymerization. *Biochem.* 46:8838–49.
 29. Chirita CN, Congdon EE, Yin H, Kuret J. (2005) Triggers of full-length tau aggregation: a role for partially folded intermediates. *Biochem.* 44:5862–72.
 30. Gamblin TC, Berry RW, Binder LI. (2003b) Tau polymerization: role of the amino terminus. *Biochem.* 42:2252–57.
 31. Kelly B, Ferreira A. (2006) Beta-amyloid-induced dynamin 1 degradation is mediated by NMDA receptors in hippocampal neurons. *J. Biol. Chem.* 281:28079–89.
 32. Czogalla A, Sikorski AF. (2005) Spectrin and calpain: a ‘target’ and a ‘sniper’ in the pathology of neuronal cells. *Cell. Mol. Life Sci.* 62:1913–24.
 33. King ME, Ahuja V, Binder LI, Kuret J. (1999) Ligand-dependent tau filament formation: implications for Alzheimer’s disease progression. *Biochem.* 38:14851–59.
 34. LeVine H. (1999) Quantification of beta-sheet amyloid fibril structures with thioflavin T. *Methods Enzymol.* 309:274–84.
 35. Santa-Maria I, Perez M, Hernandez F, Avila J, Moreno FJ. (2006) Characteristics of the binding of thioflavin S to tau paired helical filaments. *J. Alz. Dis.* 9:279–85.
 36. Yang LS, Ksiezak-Reding H. (1995) Calpain-induced proteolysis of normal human tau and tau associated with paired helical filaments. *Eur. J. Biochem.* 233:9–17.
 37. Yang LS, Gordon-Krajcer, W, Ksiezak-Reding H. (1997) Tau released from paired helical filaments with formic acid or guanidine is susceptible to calpain-mediated proteolysis. *J. Neurochem.* 69:1548–58.
 38. Biernat J, et al. (1992) The switch of tau protein to an Alzheimer-like state includes the phosphorylation of two serine-proline motifs upstream of the microtubule-binding region. *EMBO J.* 11:1593–97.
 39. Biernat J, Gustke N, Drewes G, Mandelkow E-M, Mandelkow E. (1993) Phosphorylation of Ser262 strongly reduces binding of tau to microtubules: distinction between PHF-like immunoreactivity and microtubule binding. *Neuron.* 11:153–63.
 40. Bramblett GT, et al. (1993) Abnormal tau phosphorylation at Ser 396 in Alzheimer’s disease recapitulates development and contributes to reduce microtubule binding. *Neuron.* 10:1089–99.
 41. Brion JP, Smith C, Couck AM, Gallo JM, Anderton BH. (1993) Developmental changes in tau phosphorylation: foetal tau is transiently phosphorylated in a manner similar to paired helical filament tau characteristics of Alzheimer’s disease. *J. Neurochem.* 61:2071–80.
 42. Drewes G, et al. (1992) Mitogen-activated protein (MAP) kinase transforms tau protein into an Alzheimer-like state. *EMBO J.* 6:2131–38.
 43. Drewes G, Ebneth A, Preuss U, Mandelkow E-M, Mandelkow E. (1997) MARK a novel family of protein kinases that phosphorylate microtubule-associated proteins and trigger microtubule disruption. *Cell.* 89:297–08.
 44. Goedert M, Spillatino, MG, Jakes R, Rutherford D, Crowther RA. (1989) Multiple isoforms of human microtubule-associated protein tau: sequences and localization in neurofibrillary tangles of Alzheimer’s disease. *Neuron.* 3:519–26.
 45. Goedert M, Cohen ES, Jakes R, Cohen P. (1992) p42 MAP kinase phosphorylation sites in microtubule-associated protein tau are dephosphorylated by protein phosphatase 2A1. Implications for Alzheimer’s disease. *FEBS Lett.* 312:95–99.
 46. Grunke-Iqbal I, et al. microtubule-associated protein t (tau) in Alzheimer cytoskeletal pathology. *Proc. Natl. Acad. Sci. U. S. A.* 83:4913–17.
 47. Kosik KS, Joachim CL, Selkoe DJ. (1986) Microtubule-associated protein tau (tau) is a major antigenic component of paired helical filaments in Alzheimer disease. *Proc. Natl. Acad. Sci. U. S. A.* 83:4044–48.
 48. Takashima A, Noguchi K, Sato K, Hoshimo T, Imahori K. (1993) Tau protein kinase I is essential for β -protein induced neurotoxicity. *Proc. Natl. Acad. Sci. U. S. A.* 90:7789–93.
 49. Bauman K, Mandelkow E-M, Biernat J, Pivnicka-Worms H, Mandelkow E. (1993) Abnormal Alzheimer’s like phosphorylation of tau protein by cyclin-dependent cdk2 and cdk5. *FEBS Lett.* 36:417–24.
 50. Busciglio J, Lorenzo A, Yeh J, Yankner BA. (1995) β -Amyloid fibrils induce tau phosphorylation and loss of microtubule binding. *Neuron.* 14:879–88.
 51. Hanger DP, Hughes K, Woodgett, JR, Brion JP, Anderton BH. (1992) Glycogen synthase kinase-3 induces Alzheimer’s disease-like phosphorylation of tau: generation of paired helical filament epitopes and neuronal localisation of the kinase. *Neurosci. Lett.* 147:58–62.
 52. Mandelkow E-M, et al. (1992) Glycogen synthase kinase-3 and the Alzheimer-like state of microtubule-associated protein tau. *FEBS Lett.* 314:315–21.
 53. Cho JH, Johnson GV. (2004) Glycogen synthase kinase 3 beta induces caspase-cleaved tau aggregation in situ. *J Biol. Chem.* 279:54716–23.
 54. Liu J, Liu MC, Kevin K, Wang W. (2008) Calpain in the CNS: from synaptic function to neurotoxicity. *Sci. Signal.* 1: re1 DOI 10.1126/stke.114re1.
 55. Saito K-I, Elce JS, Hamos JE, Nixon RA. (1993) Widespread activation of calcium-activated neutral proteinase (calpain) in the brain of Alzheimer’s disease: A potential molecular basis for neuronal degeneration. *Proc. Natl. Acad. Sci. U. S. A.* 90:2628–32.
 56. Lee MS, et al. (2000) Neurotoxicity induces cleavage of p35 to p25 by calpain. *Nature.* 405:360–64.
 57. Law A, Gauthier S, Quirion R. (2001) Neuroprotective and neurorescuing effects of isoform-specific nitric oxide synthase inhibitors, nitric oxide scavenger, and antioxidant against beta-amyloid toxicity. *Br. J. Pharmacol.* 133:1114–24.
 58. Vaisid T, Kosower NS, Katzav A, Chapman J, Barnoy S. (2007) Calpastatin levels affect calpain activation and calpain proteolytic activity in APP transgenic mouse model of Alzheimer’s disease. *Neurochem. Intl.* 51:391–97.
 59. Glading A, et al. (2004) Epidermal growth factor activates m-calpain (calpain II), at least in part, by extracellular signal-regulated kinase-mediated phosphorylation. *Mol. Cell. Biol.* 24:2499–2512.
 60. Zadransky, Jourdi H, Rostamiani K, Qin Q, Bi X, Baudry M. (2010) Brain-derived neurotrophic factor and epidermal growth factor activated neuronal m-calpain via mitogen-activated protein kinase-dependent phosphorylation. *J. Neurosci.* 30:1086–1095.
 61. Zadransky, Bi X, Baudry M. (2010) Regulation of calpain-2 in neurons: Implications for synaptic plasticity. *Mol. Neurobiol.* 42:143–150.
 62. Nicholson A, Riederer-Methner DN, Ferreira A (2011) Membrane cholesterol modulates beta-amyloid-dependent tau cleavage by inducing changes in the membrane content and localization of NMDA receptors. *J. Biol. Chem.* 286:976–986.
 63. Goll DE, Thompson VF, Li H, Wei W, Cong J. (2003) The calpain system. *Physiol. Rev.* 83:731–01.
 64. Rao MV, et al. (2008) Marked calpastatin (CAST) depletion in Alzheimer’s disease accelerates cytoskeleton disruption and neurodegeneration: neuroprotection by CAST overexpression. *J. Neurosci.* 28:12241–54.
 65. Garg S, Timm T, Mandelkow E-M, Mandelkow E, Wang Y. (2011) Cleavage of tau by calpain in Alzheimer’s disease: the quest for the toxic 17 kD fragment. *Neurobiol. Aging.* 32:1–14.